

Noble Metal Aerogels

International Edition: DOI: 10.1002/anie.201913079
German Edition: DOI: 10.1002/ange.201913079

Promoting the Electrocatalytic Performance of Noble Metal Aerogels by Ligand-Directed Modulation

Xuelin Fan, Swen Zerebecki, Ran Du,* René Hübner, Galina Marzum, Guocan Jiang, Yue Hu, Stephan Barcikowki, Sven Reichenberger, and Alexander Eychmüller*

Abstract: Noble metal aerogels (NMAs) are an emerging class of porous materials. Embracing nano-sized highly-active noble metals and porous structures, they display unprecedented performance in diverse electrocatalytic processes. However, various impurities, particularly organic ligands, are often involved in the synthesis and remain in the corresponding products, hindering the investigation of the intrinsic electrocatalytic properties of NMAs. Here, starting from laser-generated inorganic-salt-stabilized metal nanoparticles, various impurity-free NMAs (Au, Pd, and Au-Pd aerogels) were fabricated. In this light, we demonstrate not only the intrinsic electrocatalytic properties of NMAs, but also the prominent roles played by ligands in tuning electrocatalysis through modulating the electron density of catalysts. These findings may offer a new dimension to engineer and optimize the electrocatalytic performance for various NMAs and beyond.

Introduction

Noble metals, which are chemically inert in their bulk form, manifest unusual activities when the size is reduced to the nanoscale. Therefore, many noble-metal-based nanostructures have been extensively studied in the last few decades for various catalytic processes.^[1–3] Combining with

the unique structural features of aerogels,^[4–6] the recently appeared noble metal aerogels (NMAs) display substantial potential in catalysis.^[7,8] Because of their high stability, abundant active sites, and efficient mass/electron transfer channels, NMAs are emerging as a new class of superior electrocatalysts surpassing commercial noble-metal-based catalysts and most metal-nanoparticle (NP)-based materials.^[9,10]

Despite their exceptional performance in diverse electrocatalytic processes, such as the oxygen reduction reaction (ORR),^[11,12] ethanol oxidation reaction (EOR),^[13–15] and oxygen evolution reaction (OER),^[16] the intrinsic contribution from sole NMAs remains debated. Because a wide range of impurities may be present in aerogels, thus bringing about uncertain effects. For most fabrication approaches, wet-chemistry prepared metal NP solutions were used as precursors to yield the corresponding gels through a combined sol-gel step and drying process.^[7,8] However, to acquire stable NP solutions, particularly at a high concentrations, various organic ligands (e.g., trisodium citrates, oleic acid, and oleylamine) were inevitably involved and are difficult to be completely eliminated after synthesis.^[13,17–19] For another class of methods, that is, the freeze-casting approaches, aerogels were prepared by sequentially synthesizing NPs, concentrating by ultracentrifugation (typical final metal concentration $c_M > 300$ mM), and direct freeze drying.^[20,21] In this way, various impurities including ligands, unreacted reductants, and the products generated during preparing the NP solutions (Na^+ , BO_2^- , Cl^- , etc.) contaminate the aerogels. It was reported that noble metal gels can be prepared by directly reducing metal salt solutions (e.g. HAuCl_4 aqueous solution) with a very small amount of NaBH_4 ,^[11] thus avoiding the involvement of organic ligands. However, the gelation requires an extremely long time at room temperature (several days to several weeks). On the other hand, the presence of organic ligands is generally regarded detrimental to the catalytic process because they can block active sites and retard surface reactions.^[22,23] A few recent works have a different voice and point out their potential positive roles under certain circumstances.^[24–26] Nevertheless, the effect of different ligands in electrocatalysis and the corresponding mechanisms have not been investigated in NMA systems so far.

Laser synthesis and processing of colloids in liquids is a rather young and scalable method to prepare stable high-purity metal NP solutions free of organic ligands.^[27,28] The solution is stabilized by electrostatic repulsion between the NPs, where the surface charge arises from amphiphilic patches (e.g. OH-groups due to a partially or fully oxidized surface) or adsorbed inorganic ions.^[29,30] Inspired by this

[*] X. Fan, R. Du, G. Jiang, A. Eychmüller
Physical Chemistry, Technische Universität Dresden
Bergstr. 66b, 01069 Dresden (Germany)
E-mail: dr1581@foxmail.com
alexander.eychmueller@chemie.tu-dresden.de

S. Zerebecki, G. Marzum, S. Barcikowki, S. Reichenberger
Technical Chemistry and Center for Nanointegration Duisburg-Essen,
University of Duisburg-Essen
47057 Duisburg (Germany)

R. Hübner
Helmholtz-Zentrum Dresden-Rossendorf, Institute of Ion Beam
Physics and Materials Research
Bautzner Landstrasse 400, 01328 Dresden (Germany)

Y. Hu
College of Chemistry and Materials Engineering, Wenzhou University
Wenzhou 325000 (China)

Supporting information and the ORCID identification number(s) for the author(s) of this article can be found under:
<https://doi.org/10.1002/anie.201913079>.

© 2020 The Authors. Published by Wiley-VCH Verlag GmbH & Co. KGaA. This is an open access article under the terms of the Creative Commons Attribution Non-Commercial NoDerivs License, which permits use and distribution in any medium, provided the original work is properly cited, the use is non-commercial, and no modifications or adaptations are made.

knowledge, we propose here a strategy to fabricate impurity-free noble metal gels by destabilizing laser-generated NP colloids through the salting-out effect, where only highly-soluble small inorganic salts are involved and eventually washed-out. Using these clean gels as a platform to deliberately graft specific ligands, the ligand-directed modulation of electrocatalytic properties is unambiguously demonstrated. As will be shown by using EOR as a model reaction, the polyvinylpyrrolidone (PVP)-modified Au-Pd bimetallic aerogel delivers a prominent current density of 5.3 times higher than commercial Pd/C and 1.7 times higher than Au-Pd pristine aerogels. Besides, the underlying mechanisms are revealed by electron density modulations posed by different ligands, where the electrocatalytic activity has been positively correlated with the oxidation state of the metals. Therefore, the present work not only provides a strategy to fabricate impurity-free NMAs for probing their intrinsic properties, but also offers a new dimension for devising high-performance electrocatalysts by revisiting the effects of the ligands.

Results and Discussion

Fabrication and Characterization of Clean Noble Metal Aerogels

First, as illustrated in Figures 1a and Figure S1 in the Supporting Information, colloidal NP solutions (gold or

palladium) were prepared by a laser synthesis and processing (LSPC) method which has been reported elsewhere.^[27,28,31] In brief, laser ablation was induced by focusing a pulsed laser (wavelength 1064 nm, repetition rate 5 kHz) on an Au or Pd foil which was immersed in pure water containing 1 mM NaOH. The initially generated NPs were subsequently treated by a secondary laser processing step (wavelength 355 nm, repetition rate 50 kHz) to fragment larger particles (> 10 nm) and hence reduce the mean particle size, yielding monomodal colloidal nanoparticle solutions. As shown in Figures 1b and S2, the resulting NPs are similar to the ones produced by classical wet chemistry, displaying an average size of 4–6 nm as verified by analytical disc centrifugation analysis and transmission electron microscopy (TEM).

Various methods have been reported to destabilize noble metal NPs, such as heating, salting-out, oxidative ligand etching, and dopamine-assisted initiation.^[14,15,18,19,32,33] However, to get clean aerogels, only heating or applying highly-soluble small-size inorganic salts were attempted in this study. As seen in Figure S3, only the use of NaBH₄ can induce the gelation for all three systems (Au NPs, Pd NPs, and mixed Au NPs/Pd NPs), hence it was used in the current work. Taking the gold system as an example, the color of the original gold NP solution (metal concentration $c_M = 0.5$ mM) immediately turned red upon adding NaBH₄, and a hydrogel formed within 8 h. The corresponding monolithic aerogel was obtained by further purification and freeze-drying (Figure 1c). The gela-

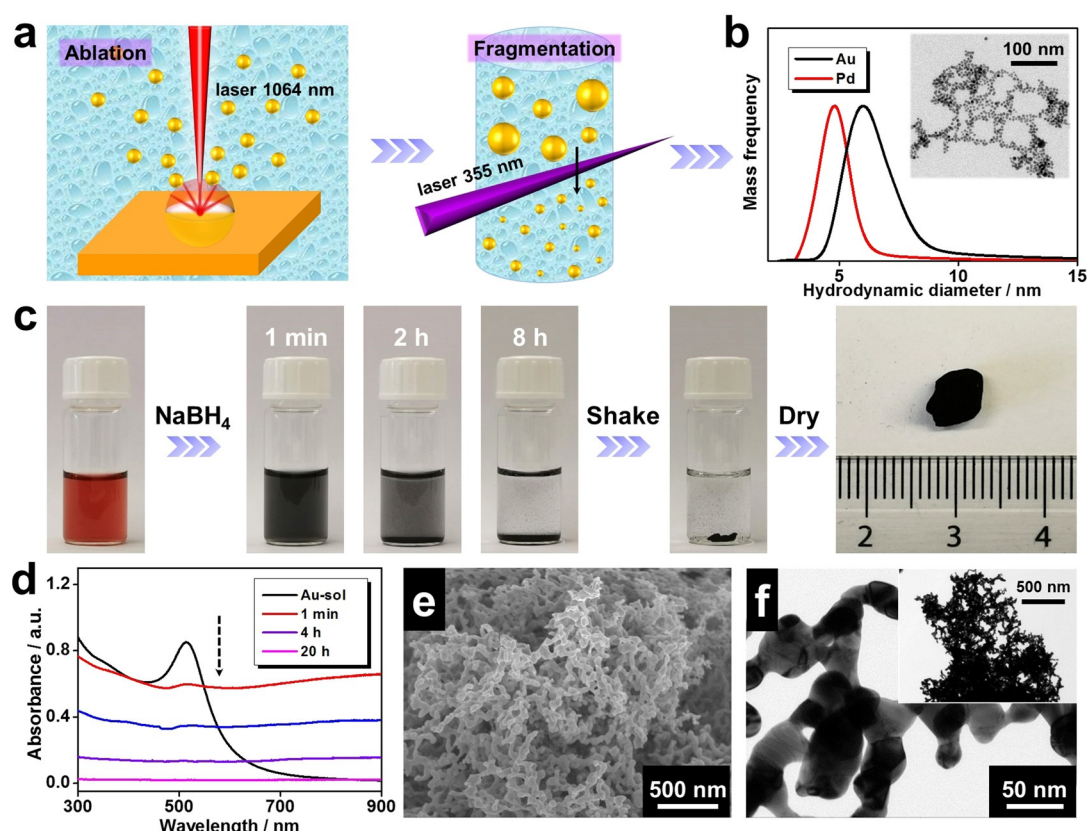


Figure 1. Fabrication of metal NPs and pristine aerogels, as well as the corresponding characterizations. a) Demonstration of colloidal metal NP preparation assisted by laser ablation and fragmentation in 1 mM NaOH aqueous solution. b) Size distribution of the as-prepared Au and Pd NPs as derived by analytical disc centrifugation. c) Fabrication process of a gold aerogel prepared from a gold NP solution. d) Time-lapse UV/Vis absorbance spectra of the Au NP solution before and after initiation. e) SEM image and f) TEM images of the obtained gold aerogel.

tion process was also monitored by in situ UV/Vis absorbance spectroscopy as shown in Figure 1d. The characteristic localized surface plasmon resonance of Au NPs centering around 510 nm instantly spanned to the entire wavelength range upon initiation and the absorbance gradually decreased afterwards, corresponding to the quick formation of nanostructured gold aggregates and their subsequent sedimentation, respectively.^[19] The morphology of the resulting gold aerogel was revealed by scanning electron microscopy (SEM) and TEM imaging (Figure 1e,f), inferring a porous structure with an average ligament size of 17.1 ± 5.5 nm.

Taking advantage of the high catalytic activity of palladium, a Pd aerogel and an Au-Pd aerogel were created by using the same route, showing similar porous structures but much smaller ligament sizes (5.9 ± 1.4 nm and 6.8 ± 0.9 nm, respectively; Figure 2a–f), which was also observed in other salting-out-induced gelation systems.^[19] Presumably because of the difference in the ligament size as well as the atomic weight, densities of the Au, Pd, and Au-Pd aerogels were estimated to be 406.4, 77.9, and 77.3 mg cm⁻³, respectively. Additionally, the nitrogen adsorption tests demonstrate high specific surface areas (SSAs) of 61.1 and 47.7 m² g⁻¹ for the Pd and Au-Pd aerogels, respectively. The pore sizes mainly reside in the mesoscale range (3–10 nm) (Figure S4). All data are summarized in Table S1. The X-ray diffraction (XRD)

patterns indicate the presence of the crystallographic phases of the corresponding metals for the two aerogels (Figure 2g). Particularly for the bimetallic Au-Pd aerogel (it is prepared by using the mixed Au NPs and Pd NPs as precursors), the XRD pattern displays separate gold and palladium diffraction peaks, suggesting that the two metals were phase-separated and not well alloyed. These findings are also supported by energy-dispersive X-ray spectroscopy (EDX) analysis, in which the two metals are separately distributed with negligible mixing at the nanoscale (Figure 2h). This is quite different from the previously reported Au-Pd aerogels where wet-chemically prepared Au NPs and Pd NPs were used as precursors,^[19,34] on which occasion that Au and Pd alloy together and occasionally overgrow each other. The reason behind this phenomenon remains to be investigated.

Modifying Noble Metal Aerogels with Ligands

Generally, ligands are regarded to be potentially harmful to catalysis because they can block active sites,^[22,23] while a few recent studies hold the opinion that many loosely-bonded ligands will not completely block the access of the reactants to the catalyst surfaces.^[25] For example, PVP-stabilized gold NPs showed an increased electron density on the Au core, facilitating electron transfer from gold to O₂ and generating super-oxo or peroxy-like species, thus promoting the aerobic oxidation of alcohols.^[24]

In another work, a specially designed tetradentate porphyrin ligand can expose large accessible sites of gold NPs and alter the reaction pathways of the electrocatalytic CO₂ reduction.^[26] For the majority of NMA systems, various organic ligands are inevitably introduced during synthesis and cannot be completely removed. Therefore, the contribution of sole NMAs is hard to evaluate, and the exact effect of the ligands is not clear. Here, in light of the surface-clean noble metal gels as prepared in this work, we have the opportunity to address these issues.

To ensure a similar morphology of the resulting materials, various ligands including trisodium citrate dihydrate (NaCA), PVP, and cetyltrimethyl ammonium bromide (CTAB) were introduced by treating pristine clean aerogels with the corresponding ligand solutions followed by appropriate washing.

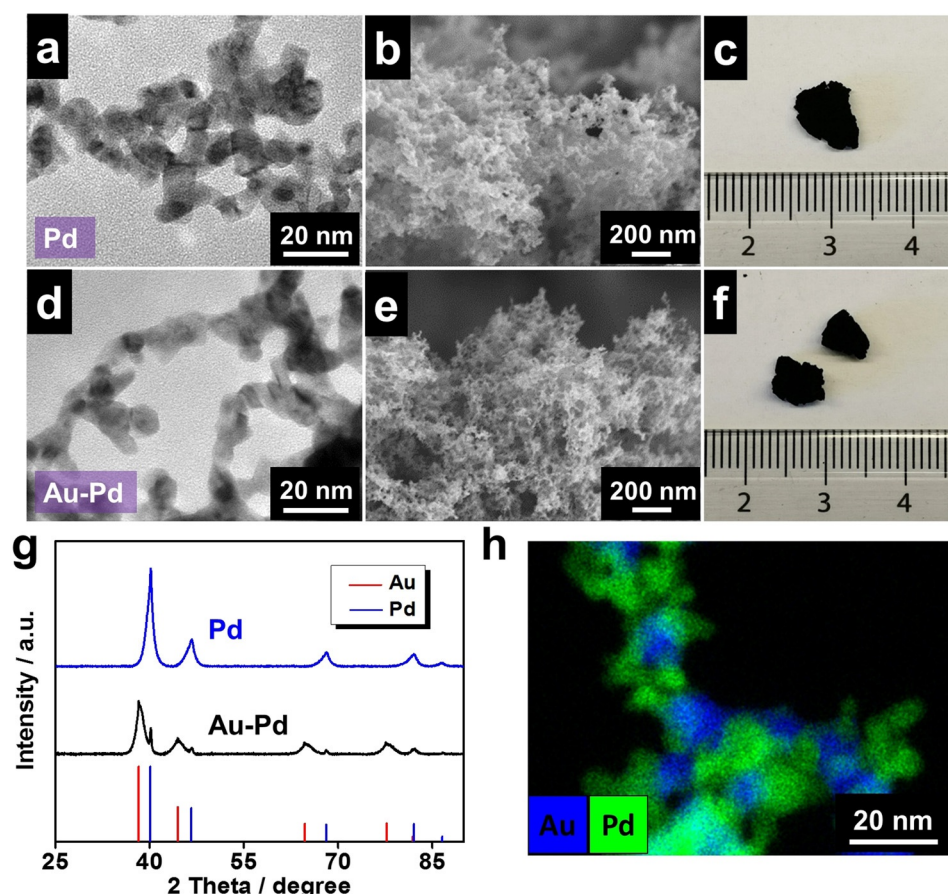


Figure 2. Characterization of pristine Pd and Au-Pd aerogels. TEM images, SEM images, and photographs of a–c) the Pd aerogel and d–f) the Au-Pd aerogel. g) XRD patterns of the Pd and Au-Pd aerogels. h) EDX mapping of the Au-Pd aerogel.

Here, the focus was placed on high-performance Au-Pd gels. Since the noble metal aerogels can substantially enhance the Raman signal due to surface-enhanced Raman scattering (SERS),^[35] Raman spectroscopy can be extremely sensitive for detecting trace amounts of ligands compared with other techniques such as Infrared (IR) spectroscopy or thermogravimetric analysis (TGA). As shown in Figure S5, the ligand-modified aerogels display peaks representing the carbon-carbon bond (present for all ligands), while no signal above the background was observed for the pristine Au-Pd aerogel, suggesting the cleanness of the pristine aerogel and the successful loading of ligands. After modification, quite similar ligament sizes were observed from TEM statistics (Figure 2 a,d, Figure S6,7).

The valence state of metals was reported to play a pivotal role in their catalytic performance. Hence, taking various Au-Pd aerogels as examples, X-ray photoelectron spectroscopy (XPS) was conducted and a deconvolution of the high-resolution Au 4f and Pd 3d spectra was performed (Figure 3 a,b, Figure S8, Table S2). The binding energies of 3d_{5/2} of Pd⁰ and Pd^{II} were assigned to 340.5 eV and 341.3 eV, while the binding energies of 4f_{7/2} of Au⁰ and Au^I were assigned to 83.9 eV and 84.4 eV, respectively.^[36,37] For pristine and NaCA-modified aerogels, the valence states of both Au and Pd are quite similar (around 6.0% Au^I and 31.0% Pd^{II}); while for PVP-modified aerogels (7.5% Au^I and 37.3% Pd^{II}) and CTAB-modified aerogels (2.5% Au^I and 28.0% Pd^{II}), the high-oxidation-state metal fraction (i.e., Au^I and Pd^{II}) is

higher and lower, respectively, compared to that of the pristine Au-Pd aerogel. Hence, this finding suggests that there might be a certain-degree of electron transfer from the gel to PVP, or from CTAB to the gel (Figure 3c). The effect of this electron density change of the aerogels on the electrocatalytic properties will be discussed in the next section.

Modulation of Electrocatalytic Properties by the Ligand Effect

Previously, NMAs have been extensively investigated for diverse electrocatalytic processes, while the effect of ligands on the catalytic performance has not been clarified so far. By taking the electrocatalytic EOR as the model reaction, pristine and various ligand-modified aerogels were probed and the corresponding mechanisms were disclosed.

As illustrated in Figure 4a, the EOR performance of commercial Pd/C, as well as that of pristine and various ligand-modified Au-Pd aerogels were characterized by cyclic voltammetry (CV). The corresponding forward current density (I_f) as well as the ratio of the forward/backward current density (I_f/I_b) were summarized. All aerogels display a considerably higher I_f than that of Pd/C (1.82 A mg_{Pd}⁻¹), indicating their high activity, while lower I_f/I_b ratios are observed for the aerogels compared to Pd/C. Considering the ligand effect, pristine aerogels exhibit a similar I_f compared to the NaCA-modified aerogel (5.72 A mg_{Pd}⁻¹ vs. 6.32 A mg_{Pd}⁻¹), while a considerable lower and higher I_f were observed for the CTAB-modified (3.15 A mg_{Pd}⁻¹) and PVP-modified Au-Pd aerogels (9.75 A mg_{Pd}⁻¹), respectively. This trend is also observed for the corresponding Pd aerogels (Figure S9a,b). Additionally, a long-term stability test marked that current retention of all Au-Pd aerogels (> 22% retention at 2000 s) considerably prevails various Pd aerogels and commercial Pd/C (< 6% retention at 2000 s), suggesting the excellent durability of the aerogel catalysts.

To reveal the underlying mechanism of this ligand-directed modulation of the electrocatalytic activity, the Au-Pd-based aerogels were selected for this study due to their high performance. Because ligand modification was performed on the same pristine aerogel by a post-treatment method, the effect of morphology can be excluded and only the change of the electronic structure may affect the catalytic properties. To this end, the I_f of various Au-Pd aerogels was correlated with

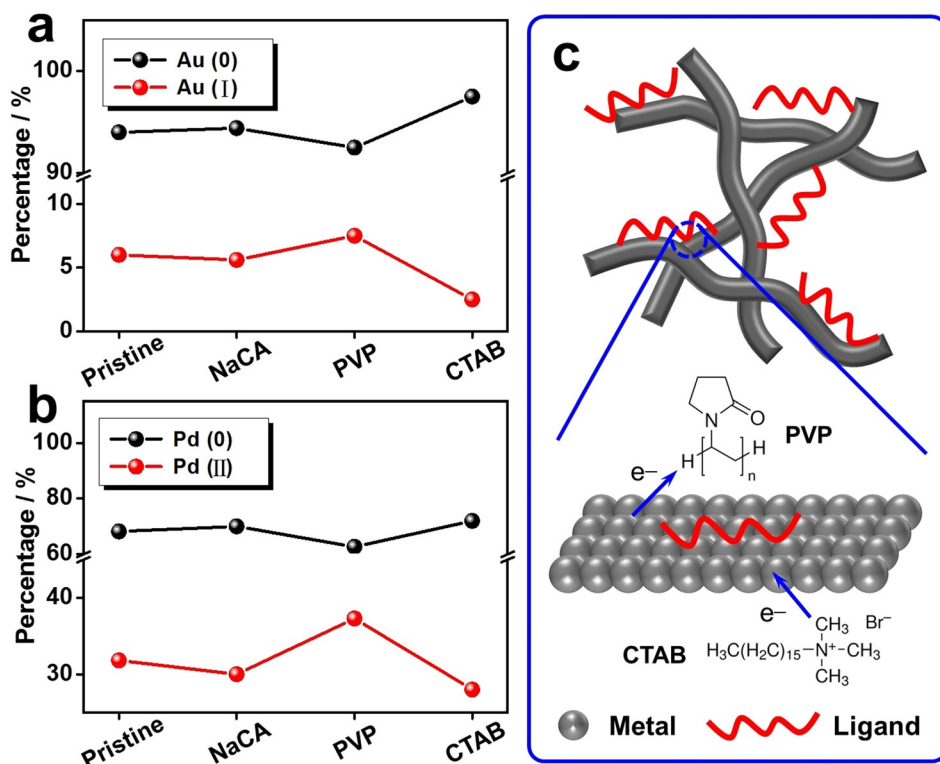


Figure 3. Valence state analysis of various ligand-modified Au-Pd aerogels. a,b) The fraction of different valence-state gold and palladium for various ligand-modified Au-Pd aerogels as derived by deconvolution of the corresponding XPS spectra. c) Schematic demonstration of the electron transfer between metals and different ligands.

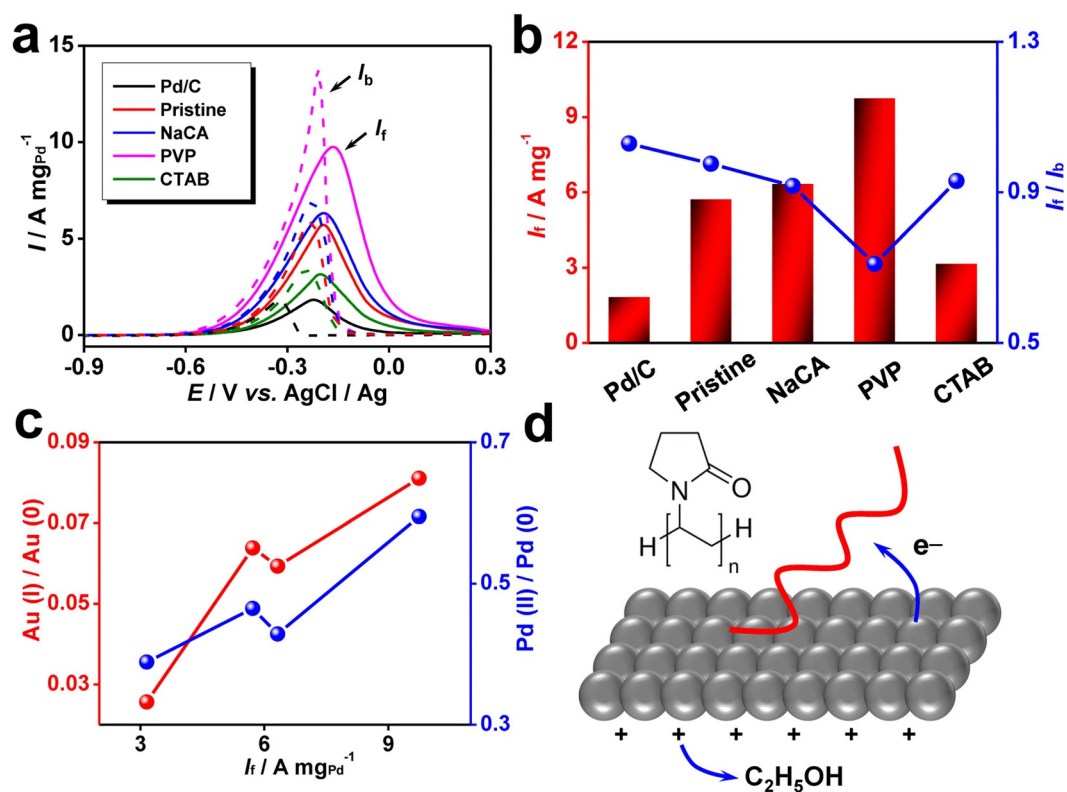


Figure 4. EOR performance of various commercial and Pd-based aerogel catalysts. a) CV curves and b) summarized I_f and I_r/I_b of Pd/C and various ligand-modified Au-Pd aerogels. c) Correlation between I_f for EOR and the oxidation states of Au and Pd. d) Proposed mechanism of the PVP-enhanced ethanol oxidation.

the Au^I/Au^0 and Pd^{II}/Pd^0 ratios As seen in Figure 4c. Generally, I_f was positively related to the ratio of high-to-low-oxidation-state species for both Au and Pd, suggesting that a higher oxidation state of the catalysts promotes the catalytic activity towards EOR. On the basis of the above results, the mechanism for the ligand-directed modulation of the electrocatalytic activity is proposed in Figure 4d. The higher oxidation state present in PVP-modified aerogels infers that a partial electron transfer from the metals to PVP occurs, thus resulting in a deficient electron density on the metals compared with other systems. In this way, the oxidation of ethanol would proceed more smoothly on these surfaces because of the presence of an extra positive potential. Thus, an enhanced EOR performance is observed. For CTAB-modified aerogels, the case inverses owing to the increased electron density on the metals compared with other systems.

Attributed to such modulation ability of the ligands, the forward current density of the PVP-modified aerogel catalysts is 5.3 times and 1.7 times higher than that of the commercial Pd/C and the pristine Au-Pd aerogel, respectively. It outperforms the previously reported Pd, Au-Pd, Cu-Pd, and Au-Ag-Pd aerogels (1.2–4.0 times higher than that of Pd/C),^[13,15,19,38] although the performance is slightly lower than those of Au-Pd-Pt and Pd-Ni hollow nanosphere aerogels (5.6–6.1 times higher than that of Pd/C).^[14,19] Moreover, the presented ligand-induced modulation method is theoretically quite

general, which may open up a potential avenue to boost the electrocatalytic performance of various catalysts.

Conclusion

To sum up, starting from laser-generated small-inorganic-salt-stabilized metal nanoparticles (NPs), ligand-free Au, Pd, and Au-Pd aerogels were readily fabricated based on the salting-out effect. Using these clean hydrogels as the platform and deliberately modifying them with specific ligands, a ligand-directed modulation of electrocatalytic properties in NMA systems was demonstrated for the first time by using ethanol oxidation as a model reaction. The PVP-modified Au-Pd aerogel was found to deliver a current density 5.3 times higher than commercial Pd/C and 1.7 times higher than the pristine aerogel. A substantially higher durability compared to Pd/C was observed for all Au-Pd aerogels. Mechanistic studies showed that specific organic ligands posed distinct effects on the electron density of the metals. Consequently, the oxidation state of the metals has been positively correlated to the catalytic activity (i.e., the current density). The deficiency of electron density can exert an extra positive potential, thus promoting the oxidation of ethanol. Therefore, the present work not only provides a scalable strategy to fabricate clean NMAs for probing their intrinsic properties, but also offers a new dimension for devising broad high-performance electrocatalysts by utilizing the ligand effect.

Data and Software Availability

All data needed to evaluate the conclusions in the paper are present in the paper and/or the Supplementary Materials. Additional data related to this paper can be requested from the authors.

Acknowledgements

R.D. acknowledges the support from the Alexander von Humboldt Foundation. We thank Shishu Zhang for assisting in the XPS measurements. The use of HZDR Ion Beam Center TEM facilities is acknowledged. This work was supported by the research funding of the Humboldt Fellowship, the ERC AdG AEROCAT, the German Federal Ministry of Education and Research (BMBF, Grant No. 03SF0451), The German federal ministry of education and research (BMBF) (KontiKat, FKZ 02P16K591), the Deutsche Forschungsgemeinschaft (DFG, German Research Foundation, 388390466–TRR 247), the National Natural Science Foundation of China (51972237), and the Natural Science Foundation of Zhejiang Province (LY19E020008).

Conflict of interest

The authors declare no conflict of interest.

Keywords: aerogels · electrocatalysis · laser · ligand · noble metals

How to cite: *Angew. Chem. Int. Ed.* **2020**, *59*, 5706–5711
Angew. Chem. **2020**, *132*, 5755–5760

-
- [1] M. Haruta, *Chem. Rec.* **2003**, *3*, 75–87.
- [2] P. K. Jain, X. Huang, I. H. El-Sayed, M. A. El-Sayed, *Acc. Chem. Res.* **2008**, *41*, 1578–1586.
- [3] Y. Xia, Y. Xiong, B. Lim, S. E. Skrabalak, *Angew. Chem. Int. Ed.* **2009**, *48*, 60–103; *Angew. Chem.* **2009**, *121*, 62–108.
- [4] N. Hüsing, U. Schubert, *Angew. Chem. Int. Ed.* **1998**, *37*, 22–45; *Angew. Chem.* **1998**, *110*, 22–47.
- [5] R. Du, Q. Zhao, N. Zhang, J. Zhang, *Small* **2015**, *11*, 3263–3289.
- [6] C. Ziegler, A. Wolf, W. Liu, A.-K. Herrmann, N. Gaponik, A. Eychmüller, *Angew. Chem. Int. Ed.* **2017**, *56*, 13200–13221; *Angew. Chem.* **2017**, *129*, 13380–13403.
- [7] R. Du, X. Fan, X. Jin, R. Hübner, Y. Hu, A. Eychmüller, *Matter* **2019**, *1*, 39–56.
- [8] R. Du, X. Jin, R. Hübner, X. Fan, Y. Hu, A. Eychmüller, *Adv. Energy Mater.* **2019**, <https://doi.org/10.1002/aenm.201901945>.
- [9] B. Cai, A. Eychmüller, *Adv. Mater.* **2019**, *31*, 1804881.
- [10] B. Cai, V. Sayevich, N. Gaponik, A. Eychmüller, *Adv. Mater.* **2018**, *30*, 1707518.
- [11] W. Liu, P. Rodriguez, L. Borchardt, A. Foelske, J. Yuan, A. K. Herrmann, D. Geiger, Z. Zheng, S. Kaskel, N. Gaponik, *Angew. Chem. Int. Ed.* **2013**, *52*, 9849–9852; *Angew. Chem.* **2013**, *125*, 10033–10037.
- [12] B. Cai, R. Hübner, K. Sasaki, Y. Zhang, D. Su, C. Ziegler, M. B. Vukmirovic, B. Rellinghaus, R. R. Adzic, A. Eychmüller, *Angew. Chem. Int. Ed.* **2018**, *57*, 2963–2966; *Angew. Chem.* **2018**, *130*, 3014–3018.
- [13] W. Liu, A. K. Herrmann, D. Geiger, L. Borchardt, F. Simon, S. Kaskel, N. Gaponik, A. Eychmüller, *Angew. Chem. Int. Ed.* **2012**, *51*, 5743–5747; *Angew. Chem.* **2012**, *124*, 5841–5846.
- [14] B. Cai, D. Wen, W. Liu, A. K. Herrmann, A. Benad, A. Eychmüller, *Angew. Chem. Int. Ed.* **2015**, *54*, 13101–13105; *Angew. Chem.* **2015**, *127*, 13293–13297.
- [15] C. Zhu, Q. Shi, S. Fu, J. Song, H. Xia, D. Du, Y. Lin, *Adv. Mater.* **2016**, *28*, 8779–8783.
- [16] Q. Shi, C. Zhu, H. Zhong, D. Su, N. Li, M. H. Engelhard, H. Xia, Q. Zhang, S. Feng, S. P. Beckman, D. Du, Y. Lin, *ACS Energy Lett.* **2018**, *3*, 2038–2044.
- [17] S. Naskar, A. Freytag, J. Deutsch, N. Wendt, P. Behrens, A. Köckritz, N. C. Bigall, *Chem. Mater.* **2017**, *29*, 9208–9217.
- [18] D. Wen, W. Liu, D. Haubold, C. Zhu, M. Oschatz, M. Holzschuh, A. Wolf, F. Simon, S. Kaskel, A. Eychmüller, *ACS Nano* **2016**, *10*, 2559–2567.
- [19] R. Du, Y. Hu, R. Hübner, J.-O. Joswig, X. Fan, A. Eychmüller, *Sci. Adv.* **2019**, *5*, eaaw4590.
- [20] H. L. Gao, L. Xu, F. Long, Z. Pan, Y. X. Du, Y. Lu, J. Ge, S. H. Yu, *Angew. Chem. Int. Ed.* **2014**, *53*, 4561–4566; *Angew. Chem.* **2014**, *126*, 4649–4654.
- [21] A. Freytag, S. Sánchez-Paradinas, S. Naskar, N. Wendt, M. Colombo, G. Pugliese, J. Poppe, C. Demirci, I. Kretschmer, D. W. Bahnemann, P. Behrens, N. C. Bigall, *Angew. Chem. Int. Ed.* **2016**, *55*, 1200–1203; *Angew. Chem.* **2016**, *128*, 1217–1221.
- [22] J. A. Lopez-Sanchez, N. Dimitratos, C. Hammond, G. L. Brett, L. Kesavan, S. White, P. Miedziak, R. Tiruvalam, R. L. Jenkins, A. F. Carley, *Nat. Chem.* **2011**, *3*, 551.
- [23] T. D. Tran, M. T. Nguyen, H. V. Le, D. N. Nguyen, Q. D. Truong, P. D. Tran, *Chem. Commun.* **2018**, *54*, 3363–3366.
- [24] H. Tsunoyama, N. Ichikuni, H. Sakurai, T. Tsukuda, *J. Am. Chem. Soc.* **2009**, *131*, 7086–7093.
- [25] G.-R. Zhang, B.-Q. Xu, *Nanoscale* **2010**, *2*, 2798–2804.
- [26] Z. Cao, S. B. Zacate, X. Sun, J. Liu, E. M. Hale, W. P. Carson, S. B. Tyndall, J. Xu, X. Liu, X. Liu, C. Song, J.-h. Luo, M.-J. Cheng, X. Wen, W. Liu, *Angew. Chem. Int. Ed.* **2018**, *57*, 12675–12679; *Angew. Chem.* **2018**, *130*, 12857–12861.
- [27] D. Zhang, B. Gökce, S. Barcikowski, *Chem. Rev.* **2017**, *117*, 3990–4103.
- [28] S. Reichenberger, G. Marzun, M. Muhler, S. Barcikowski, *ChemCatChem* **2019**, *11*, 4489–4518.
- [29] V. Merk, C. Rehbock, F. Becker, U. Hagemann, H. Nienhaus, S. Barcikowski, *Langmuir* **2014**, *30*, 4213–4222.
- [30] A. R. Zieffuß, S. Barcikowski, C. Rehbock, *Langmuir* **2019**, *35*, 6630–6639.
- [31] R. Streubel, S. Barcikowski, B. Gökce, *Opt. Lett.* **2016**, *41*, 1486–1489.
- [32] K. G. Ranmohotti, X. Gao, I. U. Arachchige, *Chem. Mater.* **2013**, *25*, 3528–3534.
- [33] X. Gao, R. J. Esteves, T. T. H. Luong, R. Jaini, I. U. Arachchige, *J. Am. Chem. Soc.* **2014**, *136*, 7993–8002.
- [34] L. Kühn, A. K. Herrmann, B. Rutkowski, M. Oezaslan, M. Nachtgeal, M. Klose, L. Giebeler, N. Gaponik, J. Eckert, T. J. Schmidt, *Chem. Eur. J.* **2016**, *22*, 13446–13450.
- [35] X. Gao, R. J. A. Esteves, L. Nahar, J. Nowaczyk, I. U. Arachchige, *ACS Appl. Mater. Interfaces* **2016**, *8*, 13076–13085.
- [36] J. F. Moulder, *Phys. Electron.* **1995**, 230–232.
- [37] M. Khawaji, D. Chadwick, *Catal. Sci. Technol.* **2018**, *8*, 2529–2539.
- [38] L. Nahar, A. A. Farghaly, R. J. A. Esteves, I. U. Arachchige, *Chem. Mater.* **2017**, *29*, 7704–7715.

Manuscript received: October 13, 2019
Version of record online: January 28, 2020